MAX-PLANCK-INSTITUT FÜR PLASMAPHYSIK

Hybrid compatible Finite Element and Finite Volume discretization for viscous and resistive MHD

Eric Sonnendrücker

MPI for Plasma Physics and Technical University of Munich

in collaboration with Francesco Fambri

Motivation

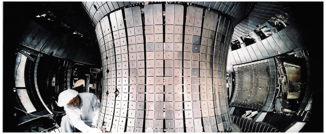
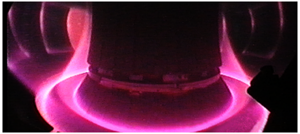
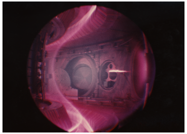
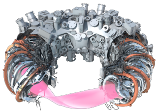

- Simulation of macroscopic dynamics for 3D magnetic confinement devices (Tokamaks and Stellerators)
- Goal: Efficient simulation of 3D nonlinear viscous and resistive MHD (VRMHD) in realistic geometry
- Conservative (mass, momentum and energy)
- Structure preserving by construction (Divergence-free; symmetry)
- Shock-capturing and robust against nonlinear instabilities
- CFL based only on the hydrodynamic convection

MHD as a non-canonical Hamiltonian system

- Many plasma (and fluid, ...) models can be expressed by an action principle or Hamiltonian systems (Morrison 1998)

$$\frac{\mathrm{d}F(\mathbf{Q})}{\mathrm{d}t} = \{F, H\}$$

- Poisson bracket encodes many invariants of the system:
  Hamiltonian H, Casimir invariants in particular $\nabla \cdot \mathbf{B}$, magnetic helicity $\int \mathbf{A} \cdot \mathbf{B} \, \mathrm{d}\mathbf{x}$, symmetry, ...
- FEEC discretization enables to obtain a finite dimensional hamiltonian system
- Idea recently applied to Vlasov-Maxwell, MHD and MHD-kinetic hybrid models.
- Issue: only works on smooth solutions. Cannot handle shocks.
- Our idea. Couple Finite Volume (FV) with FEEC, following ideas from FV community staggering some quantities.

Hamiltonian systems

- Canonical Hamiltonian system

$$\frac{\mathrm{d}\mathbf{q}}{\mathrm{d}t} = \nabla_p H, \quad \frac{\mathrm{d}\mathbf{p}}{\mathrm{d}t} = -\nabla_q H \quad \text{with } \mathbf{z} = (\mathbf{q}, \mathbf{p}): \qquad \frac{\mathrm{d}\mathbf{z}}{\mathrm{d}t} = \mathcal{J}\nabla_z H$$

$$\text{where} \quad \mathcal{J} = \begin{pmatrix} 0_N & I_N \\ -I_N & 0_N \end{pmatrix}$$

- Non canonical Hamiltonian structure with Poisson matrix $\mathcal{J}(\mathbf{z})$

$$\frac{\mathrm{d}\mathbf{z}}{\mathrm{d}t} = \mathcal{J}(\mathbf{z})\nabla_z H, \quad \text{Poisson bracket:} \quad \{F, G\} = (\nabla_z F)\mathcal{J}(\mathbf{z})\nabla_z G$$

- Also in infinite dimensional case replacing gradient by functional derivative and where $\mathcal{J}$ is a differential operator

$$\frac{\mathrm{d}U}{\mathrm{d}t} = \mathcal{J}(U)\frac{\delta\mathcal{H}}{\delta U}$$

- $\mathcal{J}$ can be degenerate: C s.t. $\mathcal{J}(U)\frac{\delta\mathcal{C}}{\delta U} = 0$ are Casimir invariants.

Gradient flows

- Dissipative systems with increase of entropy or dissipation of free energy

$$\frac{\mathrm{d}U}{\mathrm{d}t} = -\mathcal{K}(U)\frac{\delta \mathcal{S}}{\delta U}$$

- $\mathcal{K}(U)$ is a possibly degenerate semi-positive operator hence:

$$\frac{\mathrm{d}\mathcal{S}(U)}{\mathrm{d}t} = -\frac{\delta \mathcal{S}}{\delta U} \cdot \mathcal{K}(U)\frac{\delta \mathcal{S}}{\delta U} \leq 0.$$

- Choose dissipation mechanism $\mathcal{K}(U)$ and dissipated functional $\mathcal{S}$, *e.g*
  1. Heat equation: $\mathcal{S} = \int \log T$
  2. Particle collisions: $\mathcal{S} = k_B \int f \log f$

Combining hamiltonian and dissipative dynamics

- Dynamical systems arising in physics often combine a hamiltonian and a dissipative part
- Introducing a hamiltonian $\mathcal{H}$ which is conserved and a free energy (or entropy) $\mathcal{S}$ which is dissipated,

$$\frac{\mathrm{d}\mathcal{F}}{\mathrm{d}t} = \{\mathcal{F}, \mathcal{H}\} - (\mathcal{F}, \mathcal{S}) \qquad \equiv \qquad \frac{\mathrm{d}U}{\mathrm{d}t} = \mathcal{J}(U)\frac{\delta \mathcal{H}}{\delta U} - \mathcal{K}(U)\frac{\delta \mathcal{S}}{\delta U}$$

  with $\mathcal{J}$ a Poisson operator and $\mathcal{K}$ a symmetric semi-definite positive operator, $\mathcal{F}, \mathcal{S}, \mathcal{H}$ functionals of U.
- Entropy is preserved by Poisson bracket and energy is preserved by dissipative bracket

$$\{\mathcal{S}, \mathcal{H}\} = 0, \qquad (\mathcal{H}, \mathcal{S}) = 0.$$

$\Rightarrow$ Exact energy preservation and production of entropy

$$\frac{\mathrm{d}\mathcal{H}}{\mathrm{d}t} = \{\mathcal{H}, \mathcal{H}\} - (\mathcal{H}, \mathcal{S}) = 0, \qquad \frac{\mathrm{d}\mathcal{S}}{\mathrm{d}t} = \{\mathcal{S}, \mathcal{H}\} - (\mathcal{S}, \mathcal{S}) \leq 0.$$

Example: the Vlasov-Maxwell-Landau kinetic model

$$\frac{\partial f}{\partial t} + \mathbf{v} \cdot \nabla_x f + \frac{q}{m}(\mathbf{E} + \mathbf{v} \times \mathbf{B}) \cdot \nabla_v f = Q(f, f)$$

- Fits into the metriplectic framework

$$\frac{d}{dt}\mathcal{F} = \{\mathcal{F}, \mathcal{H}\} + (\mathcal{F}, \mathcal{S}), \quad \mathcal{S} = \int f \ln f \, \mathrm{d}\mathbf{x} \, \mathrm{d}\mathbf{v}$$

$$\mathcal{H} = \frac{m}{2} \int f v^2 \, \mathrm{d}\mathbf{x} \, \mathrm{d}\mathbf{v} + \frac{\epsilon_0}{2} \int E^2 \, \mathrm{d}\mathbf{x} + \frac{1}{2\mu_0} \int B^2 \, \mathrm{d}\mathbf{x}$$

- Metriplectic bracket preserves mass, momentum, total energy, divergence constraints on E and B, and satisfies an H-theorem (monotonic dissipation of entropy, unique equilibrium state)
- discretisation of the brackets instead of the dynamical equation guarantees these properties at the discrete level and can be achieved by different numerical methods (FEM, DG, PIC,...)

Coming back to MHD

- Couple Finite Element Exterior Calculus to handle symmetric terms appearing in brackets and robust shock capturing Finite Volume scheme for convection.
- Features of our problem:
  - high characteristic wave speeds
  - high mesh resolution

  $\Longrightarrow$ computational time-step Δt severely constrained by CFL (Alfvén and magnetosonic speeds)
- Implicit or semi-implicit methods are a must. Computationally efficient and robust methods for long-time simulations of 3D plasma flows

- Explicit high-order FV or DG for convection
- Implicit Structure Preserving Finite Elements for acoustic and Alfvénic steps

First implementation: low order FV/FEEC on Cartesian grids
Ongoing implementation: high-order FV and FEEC in AMReX framework (block structured AMR on cartesian grids)
$\rightsquigarrow$ Performance portability on novel architectures including different kinds of GPU

Governing equations (VRMHD) in conservative form

The viscous and resistive MHD equations can be cast in the following conservative form

$$\frac{\partial}{\partial t}\mathbf{Q} + \nabla \cdot (\mathbf{F} - \mathbf{F}_d) = 0 \tag{1}$$

$$\mathbf{Q} := \begin{pmatrix} \rho \\ \rho\mathbf{v} \\ \rho E \\ \mathbf{B} \end{pmatrix}; \quad \mathbf{F} = \mathbf{F}(\mathbf{Q}) := \begin{pmatrix} \rho\mathbf{v} \\ \rho\mathbf{v}\otimes\mathbf{v} + \left(p + \frac{\mathbf{B}^2}{2}\right)\mathbf{I} - \mathbf{B}\otimes\mathbf{B} \\ \left(\rho E + p + \frac{1}{2}\mathbf{B}^2\right)\mathbf{v} - \mathbf{B}\left(\mathbf{v}\cdot\mathbf{B}\right) \\ \mathbf{B}\otimes\mathbf{v} - \mathbf{v}\otimes\mathbf{B} \end{pmatrix} \tag{2}$$

$$\mathbf{F}_d = \mathbf{F}_d(\mathbf{Q}, \nabla\mathbf{Q}) := \begin{pmatrix} 0 \\ \mu\left(\nabla\mathbf{v} + \nabla\mathbf{v}^T - \frac{2}{3}\left(\nabla\cdot\mathbf{v}\right)\mathbf{I}\right) \\ \mu\mathbf{v}\left(\nabla\mathbf{v} + \nabla\mathbf{v}^T - \frac{2}{3}\left(\nabla\cdot\mathbf{v}\right)\mathbf{I}\right) + \kappa\nabla T + \frac{\eta}{4\pi}\mathbf{B}\left(\nabla\mathbf{B} - \nabla\mathbf{B}^T\right) \\ \eta\left(\nabla\mathbf{B} - \nabla\mathbf{B}^T\right) \end{pmatrix} \tag{3}$$

with the identity matrix $\mathbf{I}$, T is the temperature that refers to a thermal equation of state $T = T(p, \rho)$, μ is the kinematic viscosity, κ is the thermal conductivity and η is the electric resistivity of the fluid.

Ideal MHD: characteristics wave speeds

Considering ideal plasma flow in one single space dimension:

$$\frac{\partial \mathbf{Q}}{\partial t} + \frac{\partial \mathbf{F}}{\partial x} = 0. \tag{4}$$

For $B_x = const.$ one can easily compute its eight eigenvalues

$$\lambda_{1,8}^{\text{MHD}} = u \mp c_f, \quad \lambda_{2,7}^{\text{MHD}} = u \mp c_a, \quad \lambda_{3,6}^{\text{MHD}} = u \mp c_s, \quad \lambda_4^{\text{MHD}} = u, \quad \lambda_5^{\text{MHD}} = 0, \tag{5}$$

where

$$\begin{aligned} c_a &= B_x/\sqrt{4\pi\rho} && \textit{Alfvén speed}, \\ c_s^2 &= \tfrac{1}{2}\left(b^2 + c^2 - \sqrt{(b^2+c^2)^2 - 4c_a^2c^2}\right) && \textit{slow magnetosonic}, \\ c_f^2 &= \tfrac{1}{2}\left(b^2 + c^2 + \sqrt{(b^2+c^2)^2 - 4c_a^2c^2}\right) && \textit{fast magnetosonic}. \end{aligned} \tag{6}$$

c: adiabatic sound speed: (EOS) $p = p(e,\rho)$ as $c^2 = \partial p/\partial\rho + p/\rho^2 \partial p/\partial e$, e.g. $c^2 = \gamma p/\rho$ for the ideal gas EOS. $b^2 = \mathbf{B}^2/\rho$.

Splitting between slow and fast parts

- In a magnetic fusion plasma convection is slow, but other waves very fast.
- We split the flux in 3 parts $\mathbf{F} = \mathbf{F}_v + \mathbf{F}_p + \mathbf{F}_b$ with

$$\mathbf{Q} := \begin{pmatrix} \rho \\ \rho\mathbf{v} \\ \rho E \\ \mathbf{B} \end{pmatrix}; \quad \mathbf{F}_v := \begin{pmatrix} \rho\mathbf{v} \\ \rho\mathbf{v}\otimes\mathbf{v} \\ \frac{1}{2}\mathbf{v}\rho\mathbf{v}^2 \\ 0 \end{pmatrix} \quad \mathbf{F}_p := \begin{pmatrix} 0 \\ p\mathbf{I} \\ \frac{\gamma}{\gamma-1}p\mathbf{v} \\ 0 \end{pmatrix} \quad \mathbf{F}_b := \begin{pmatrix} 0 \\ (\frac{1}{2}\mathbf{B}^2\mathbf{I} - \mathbf{B}\otimes\mathbf{B}) \\ \mathbf{v}\mathbf{B}^2 - (\mathbf{v}\cdot\mathbf{B})\mathbf{B} \\ \mathbf{B}\otimes\mathbf{v} - \mathbf{v}\otimes\mathbf{B} \end{pmatrix} \tag{7}$$

as $\rho E + p + \frac{1}{2}\mathbf{B}^2 = \frac{\gamma}{\gamma-1}p + \frac{1}{2}\rho\mathbf{v}^2 + \mathbf{B}^2$ for a perfect gas.

- **Convection step** ($\mathbf{F}_v$) explicit, **acoustic** and **Alfvénic steps** ($\mathbf{F}_p$ and $\mathbf{F}_b$) implicit
- Properties:
  - Magnetic field $\mathbf{B}$ stays constant in convection and acoustic steps.
  - Density ρ stays constant in acoustic and Alfvénic steps.
  - Energy ρE is decoupled from $\mathbf{v}$ and $\mathbf{B}$ in Alfvénic step.

Characteristic wave speeds for split parts

$i)$ explicit (Convection) $\quad \partial_t \mathbf{Q} + \partial_x \mathbf{F}_v = 0,$

$$\lambda^v_{1,2,3,4} = 0, \quad \lambda^v_{5,6,7,8} = v_x, \tag{8}$$

$ii)$ implicit (Acoustic) $\quad \partial_t \mathbf{Q} + \partial_x \mathbf{F}_p = 0,$

$$\lambda^p_{1,8} = \frac{1}{2}\left(v_x \mp \sqrt{v_x^2 + 4c^2}\right), \tag{9}$$

ToroVazquez2012

$$\lambda^p_{2,3,4,5,6,7} = 0,$$

$iii)$ implicit (Alfvénic) $\quad \partial_t \mathbf{Q} + \partial_x \mathbf{F}_b = 0.$

$$\lambda^B_{1,8} = \frac{1}{2}\left(v_x \mp \sqrt{v_x^2 + 4\left(\frac{|\mathbf{B}|}{\sqrt{4\pi\rho}}\right)^2}\right), \tag{10}$$

Fambri2021

$$\lambda^B_{2,7} = \frac{1}{2}\left(v_x \mp \sqrt{v_x^2 + 4\left(\frac{B_x}{\sqrt{4\pi\rho}}\right)^2}\right),$$

$$\lambda^B_{3,4,5,6} = 0.$$

3-split time-integration (VRMHD)

The summary of the chosen split systems will be

$$\partial_t \mathbf{Q} + \nabla \cdot \mathbf{F} = 0, \qquad \mathbf{F} := (\mathbf{F}_v - \mathbf{F}_\mu) \qquad \textit{Explicit in time} \tag{11}$$

$$+ (\mathbf{F}_b - \mathbf{F}_\eta) \qquad \textit{Implicit in time} \tag{12}$$

$$+ \mathbf{F}_p. \qquad \textit{Implicit in time} \tag{13}$$

Implicit steps will be based on Finite Element Exterior Calculus spaces to enforce $\nabla \cdot \mathbf{B} = 0$ and keep the symmetries needed for efficient implicit solves.
Finite Volume variables (***dual*-cell** averages, centered in the *nodes* of the main grid):

$$\rho, \quad \mathbf{m} = \rho \mathbf{v}, \quad \rho E$$

Finite Element variables (in appropriate Finite Element spaces)

$$\mathbf{m}_e, \quad \mathbf{p}, \quad \mathbf{B}_f$$

Note that $\mathbf{B}_f$ is a purely Finite Element variable, $\mathbf{m}$ is a Finite Volume variable, which has a corresponding Finite Element variable $\mathbf{m}_e$.

(I) Explicit terms: nonlinear convection and viscous subsystems

The chosen procedure for discretizing the nonlinear convection and the viscous terms that are summarized in the first subsystem

$$\partial_t \mathbf{Q} + \nabla \cdot (\mathbf{F}_v - \mathbf{F}_\mu) = 0 \tag{14}$$

A **conservative explicit finite-volume scheme** of the type

$$\begin{aligned} \mathbf{Q}^*_{i,j,k} = \mathbf{Q}^n_{i,j,k} \quad & -\frac{\Delta t}{\Delta x}\left(\mathbf{f}_{i+\frac{1}{2},j,k} - \mathbf{f}_{i-\frac{1}{2},j,k}\right) - \frac{\Delta t}{\Delta y}\left(\mathbf{g}_{i,j+\frac{1}{2},k} - \mathbf{g}_{i,j-\frac{1}{2},k}\right) + \\ & -\frac{\Delta t}{\Delta z}\left(\mathbf{h}_{i,j,k+\frac{1}{2}} - \mathbf{h}_{i,j,k-\frac{1}{2}}\right), \end{aligned} \tag{15}$$

is adopted, where the star symbol * is used to indicate that $\mathbf{Q}^*$ is only a local solution of sub-system (I). In particular, one has numerical (**Rusanov**, or **local Lax-Friedrichs**) fluxes of the type

$$\begin{aligned} \mathbf{f}_{i+\frac{1}{2},j,k} := \quad & \frac{1}{2}\left(\mathbf{F}_v(\mathbf{Q}^-_{i+\frac{1}{2},j,k}) + \mathbf{F}_v(\mathbf{Q}^+_{i+\frac{1}{2},j,k})\right) - \frac{1}{2} s^x_{\max}\left(\mathbf{Q}^+_{i+\frac{1}{2},j,k} - \mathbf{Q}^-_{i+\frac{1}{2},j,k}\right) + \\ & -\left\{\left\langle \mathbf{F}_\mu(\mathbf{V}_h, \nabla \mathbf{V}_h)\right\rangle_{yz}\right\}_{i+\frac{1}{2},j,k} \end{aligned} \tag{16}$$

Symmetric formulations of acoustic and Alfvénic systems

- In the **Acoustic step** ρ and $\mathbf{B}$ are constant, so that we solve for $\mathbf{m} = \rho\mathbf{v}$ and p

$$\frac{\partial \mathbf{m}}{\partial t} + \nabla p = 0 \tag{17}$$

$$\frac{\partial}{\partial t}\left(\frac{p}{\gamma - 1} + \frac{1}{2\rho}\mathbf{m}^2\right) + \frac{\gamma}{\gamma - 1}\nabla \cdot \left(\frac{p}{\rho}\mathbf{m}\right) = 0 \tag{18}$$

- The **Alfvénic step** involves a coupled system in $\mathbf{m}$ and $\mathbf{B}$

$$\frac{\partial \mathbf{m}}{\partial t} - (\nabla \times \mathbf{B}) \times \mathbf{B} = 0 \tag{19}$$

$$\frac{\partial \mathbf{B}}{\partial t} - \nabla \times \left(\frac{1}{\rho}\mathbf{m} \times \mathbf{B}\right) + \eta\nabla \times (\nabla \times \mathbf{B}) = 0 \tag{20}$$

and a decoupled energy equation:

$$\frac{\partial \rho E}{\partial t} + \nabla \cdot \frac{1}{\rho}\left(\mathbf{B}^2\mathbf{m} - (\mathbf{m} \cdot \mathbf{B})\mathbf{B}\right) = 0. \tag{21}$$

Finite Element Exterior Calculus

Acoustic and Alfvénic steps will be discretized with compatible Finite Elements . These are based on the following commuting diagram involving a continuous and a discrete deRham complex as well as commuting projectors:

$$\begin{tikzcd}
H^1(\Omega) \arrow[r, "\mathrm{grad}"] \arrow[d, "\Pi_0"'] & H(\mathrm{curl},\Omega) \arrow[r, "\mathrm{curl}"] \arrow[d, "\Pi_1"'] & H(\mathrm{div},\Omega) \arrow[r, "\mathrm{div}"] \arrow[d, "\Pi_2"'] & L^2(\Omega) \arrow[d, "\Pi_3"'] \\
V_0 \arrow[r, shift left, "\mathrm{grad}"] & V_1 \arrow[l, shift left, "\mathrm{div}_w"] \arrow[r, shift left, "\mathrm{curl}"] & V_2 \arrow[l, shift left, "\mathrm{curl}_w"] \arrow[r, shift left, "\mathrm{div}"] & V_3 \arrow[l, shift left, "\mathrm{grad}_w"]
\end{tikzcd}$$

where the weak discrete differential operators are defined by

$$\int \mathrm{grad}\, p_h \cdot \mathbf{v}_h \, \mathrm{d}\mathbf{x} = -\int \mathrm{div}_w \, \mathbf{v}_h \cdot p_h \, \mathrm{d}\mathbf{x}, \quad p_h \in V_0, \mathbf{v}_h \in V_1, \tag{22}$$

$$\int \mathrm{curl}\, \mathbf{u}_h \cdot \mathbf{B}_h \, \mathrm{d}\mathbf{x} = \int \mathrm{curl}_w \, \mathbf{B}_h \cdot \mathbf{u}_h \, \mathrm{d}\mathbf{x}, \quad \mathbf{B}_h \in V_2, \mathbf{u}_h \in V_1, \tag{23}$$

$$\int q_h \mathrm{div}\, \mathbf{B}_h \, \mathrm{d}\mathbf{x} = -\int \mathrm{grad}_w \, q_h \cdot \mathbf{B}_h \, \mathrm{d}\mathbf{x}, \quad q_h \in V_3, \mathbf{B}_h \in V_2, \tag{24}$$

Example: two options for linearized acoustics

$$\begin{aligned} \frac{\partial \mathbf{u}}{\partial t} + \nabla p = 0 \\ \frac{\partial p}{\partial t} + \nabla \cdot \mathbf{u} = 0 \end{aligned} \tag{25}$$

$$\begin{tikzcd} H^1(\Omega) \arrow[r, "\mathrm{grad}"] \arrow[d, "\Pi_0"'] & H(\mathrm{curl}, \Omega) \arrow[d, "\Pi_1"] \\ V_0 \arrow[r, shift left, "\mathrm{grad}"] & V_1 \arrow[l, shift left, "\mathrm{div}_w"] \end{tikzcd}
\qquad
\begin{tikzcd} H(\mathrm{div}, \Omega) \arrow[r, "\mathrm{div}"] \arrow[d, "\Pi_2"'] & L^2(\Omega) \arrow[d, "\Pi_3"] \\ V_2 \arrow[r, shift left, "\mathrm{div}"] & V_3 \arrow[l, shift left, "\mathrm{grad}_w"] \end{tikzcd}$$

1. $p_h \in V_0$, $\mathbf{u}_h \in V_1$

$$\frac{\partial \mathbf{u}_h}{\partial t} + \nabla p_h = 0 \tag{26}$$

$$\frac{\mathrm{d}}{\mathrm{d}t} \int p_h q_h \,\mathrm{d}x - \int \mathbf{u}_h \cdot \nabla q_h \,\mathrm{d}x = 0 \quad \forall q_h \in V_0 \quad \left(\frac{\partial p_h}{\partial t} + \nabla_w \cdot \mathbf{u}_h = 0 \right) \tag{27}$$

2. $p_h \in V_3$, $\mathbf{u}_h \in V_2$

$$\frac{\mathrm{d}}{\mathrm{d}t} \int \mathbf{u}_h \cdot \mathbf{v}_h \,\mathrm{d}x - \int p_h \nabla \cdot \mathbf{v}_h \,\mathrm{d}x = 0 \quad \forall \mathbf{v}_h \in V_2 \quad \left(\frac{\partial \mathbf{u}_h}{\partial t} + \nabla_w p_h = 0 \right) \tag{28}$$

$$\frac{\partial p_h}{\partial t} + \nabla \cdot \mathbf{u}_h = 0 \tag{29}$$

Choice of the Finite Element spaces (Acoustic and Alfvén steps)

Both systems involve two coupled equations involving differential operators and their dual

- grad and $-\mathrm{div}$ for the acoustic step
- curl and curl for the Alfvénic step

In the context of FEEC one of these must be treated strongly and the other one weakly. This holds at the discrete level with appropriate choice of Finite Element spaces.
Two natural choices

1. $p \in V_0$ (node), $\mathbf{m} \in V_1$ (edge), $\mathbf{B} \in V_2$ (face)
   - $\mathbf{B}$ strongly divergence free, strong momentum equation
   - Discretization of resistive term more "complicated".
2. $p \in V_3$ (volume), $\mathbf{m} \in V_2$ (face), $\mathbf{B} \in V_1$ (edge)
   - $\mathbf{B}$ weakly divergence free
   - Discretization of resistive term straightforward

We choose a hybrid option : ideal MHD step on a main grid (strong div), resistive step on a dual grid (strong curl).

Discrete differential operators in matrix form

Equations in strong form can be expressed directly as an algebraic relation between the degrees of freedom:

$$\mathbf{u}_e = \nabla\varphi, \quad \text{for } \varphi \in V_0, \mathbf{u}_e \in V_1 \quad \Longleftrightarrow \quad \mathbf{U}_e = \mathbb{G}\boldsymbol{\varphi}$$

Applying the weak differential operators, involves the inversion of a mass matrix:
$\mathbb{G}$, $\mathbb{C}$, $\mathbb{D}$: discrete strong differential operators;
$\tilde{\mathbb{G}}$, $\tilde{\mathbb{C}}$, $\tilde{\mathbb{D}}$: weak differential operators;
$\mathbb{M}_i$ for $i = 0, 1, 2, 3$: mass matrix of V_i.

$$\Sigma_0 \underset{\tilde{\mathbb{D}}}{\overset{\mathbb{G}}{\rightleftarrows}} \Sigma_1 \underset{\tilde{\mathbb{C}}}{\overset{\mathbb{C}}{\rightleftarrows}} \Sigma_2 \underset{\tilde{\mathbb{G}}}{\overset{\mathbb{D}}{\rightleftarrows}} \Sigma_3$$

$$\mathbb{M}_2\tilde{\mathbb{G}} = -\mathbb{D}^\top\mathbb{M}_3, \quad \mathbb{M}_1\tilde{\mathbb{C}} = \mathbb{C}^\top\mathbb{M}_2, \quad \mathbb{M}_0\tilde{\mathbb{D}} = -\mathbb{G}^\top\mathbb{M}_1. \tag{30}$$

Important property:

	discrete *primal* sequence	discrete *dual* sequence
$curl \circ grad = 0$	$\mathbb{C}\mathbb{G} = 0$	$\tilde{\mathbb{C}}\tilde{\mathbb{G}} = 0$
$div \circ curl = 0$	$\mathbb{D}\mathbb{C} = 0$	$\tilde{\mathbb{D}}\tilde{\mathbb{C}} = 0$

Special case: low order and Cartesian grid

We consider in this talk low order Finite Elements: Let us denote by $\varphi_{i-\frac{1}{2}}(x)$ the linear hat functions associated to the node $x_{i-\frac{1}{2}}$ in 1D

$$\varphi_{i-\frac{1}{2}}(x) = \begin{cases} \frac{x-x_{i-\frac{3}{2}}}{\Delta x} & x_{i-\frac{3}{2}} \leq x \leq x_{i-\frac{1}{2}} \\ -\frac{x-x_{i+\frac{1}{2}}}{\Delta x} & x_{i-\frac{1}{2}} \leq x \leq x_{i+\frac{1}{2}} \\ 0 & \text{else} \end{cases}$$

and by χ_i the piecewise constant basis functions in 1D

$$\chi_i(x) = \begin{cases} 1 & x_{i-\frac{1}{2}} \leq x \leq x_{i+\frac{1}{2}} \\ 0 & \text{else} \end{cases}$$

- Then functions in V_0, V_1, V_2, V_3 **can be expressed as tensor product bases.**
- e.g, $V_0 = \mathbb{Q}_1$ the tensor product piecewise linear element (Lagrange Polynomials);
- e.g., $V_3 = \mathbb{Q}_0$, piecewise constant;
- V_1 and V_2, “mixed” tensor product spaces...

Special case: low order and Cartesian grid

For any $p_h \in V_0$ $\qquad p_h(x,y,z) = \sum_{i,j,k} p_{i-\frac{1}{2},j-\frac{1}{2},k-\frac{1}{2}} \varphi_{i-\frac{1}{2}}(x)\varphi_{j-\frac{1}{2}}(y)\varphi_{k-\frac{1}{2}}(z),$

for any $\mathbf{u}_h \in V_1 = V_1^x \times V_1^y \times V_1^z$

$$u_{h,x}(x,y,z) = \sum_{i,j,k} (u_{e,x})_{i,j-\frac{1}{2},k-\frac{1}{2}} \chi_i(x)\varphi_{j-\frac{1}{2}}(y)\varphi_{k-\frac{1}{2}}(z),$$

$$u_{h,y}(x,y,z) = \sum_{i,j,k} (u_{e,y})_{i-\frac{1}{2},j,k-\frac{1}{2}} \varphi_{i-\frac{1}{2}}(x)\chi_j(y)\varphi_{k-\frac{1}{2}}(z),$$

$$u_{h,z}(x,y,z) = \sum_{i,j,k} (u_{e,z})_{i-\frac{1}{2},j-\frac{1}{2},k} \varphi_{i-\frac{1}{2}}(x)\varphi_{j-\frac{1}{2}}(y)\chi_k(z),$$

for any $\mathbf{B}_h \in V_2 = V_2^x \times V_2^y \times V_2^z$

$$B_{h,x}(x,y,z) = \sum_{i,j,k} (B_{f,x})_{i-\frac{1}{2},j,k} \varphi_{i-\frac{1}{2}}(y)\chi_j(x)\chi_k(z),$$

$$B_{h,y}(x,y,z) = \sum_{i,j,k} (B_{f,y})_{i,j-\frac{1}{2},k} \chi_i(x)\varphi_{j-\frac{1}{2}}(y)\chi_k(z),$$

$$B_{h,z}(x,y,z) = \sum_{i,j,k} (B_{f,z})_{i,j,k-\frac{1}{2}} \chi_i(x)\chi_j(y)\varphi_{k-\frac{1}{2}}(z),$$

and for any $q_h \in V_3$ $\qquad q_h(x,y,z) = \sum_{i,j,k} q_{i,j,k} \chi_i(x)\chi_j(y)\chi_k(z).$

Location of FEEC degrees of freedom

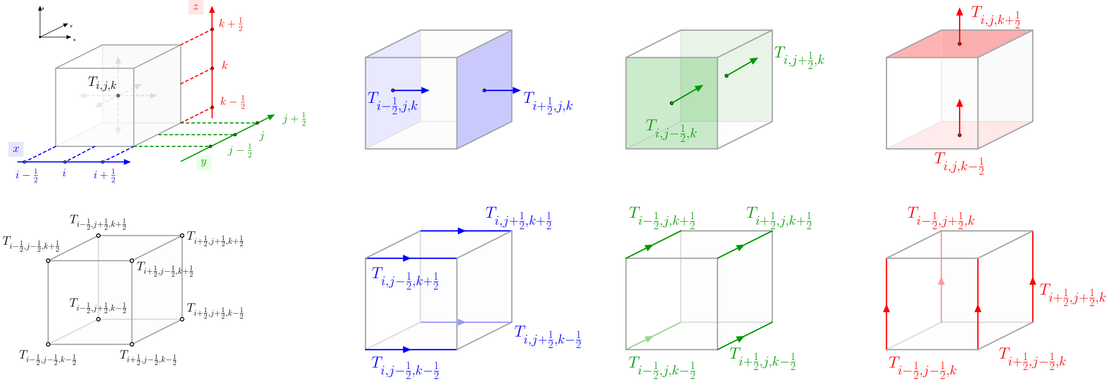

Figure: Barycenters (top left), vertices (bottom left), faces (3 components, top right) and edges (3 components, bottom right) on a three-dimensional Cartesian structured grid.

$$\rho_n, \rho\mathbf{v}_n, \rho E_n, p_n \in V_0(\text{nodes}) \qquad \mathbf{m}_e, \mathbf{v}_e \in V_1(\text{edges}) \qquad \mathbf{B}_f \in V_2(\text{faces})$$

Special case: low order and Cartesian grid

- Approximating integrals in mass matrices (complex based on $\mathbb{Q}_1$) with the trapezoidal rule:

$$\mathbb{M}_0 = \mathbb{M}_3 = \Delta x \Delta y \Delta z \mathbb{I}_N, \quad \mathbb{M}_1 = \mathbb{M}_2 = \Delta x \Delta y \Delta z \mathbb{I}_{3N}.$$

This implies that the relation between primal and dual differential operators (30) becomes

$$\tilde{\mathbb{G}} = -\mathbb{D}^\top, \;\; \tilde{\mathbb{C}} = \mathbb{C}^\top, \;\; \tilde{\mathbb{D}} = -\mathbb{G}^\top. \tag{31}$$

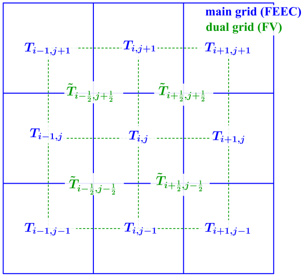

- In this case discrete expression between degrees of freedom is equivalent to Finite Differences on staggered meshes, e.g.

$$(\mathbb{G}\mathbf{P})_i^x = (p_{i+\frac{1}{2}} - p_{i-\frac{1}{2}})/\Delta x$$

(II) Implicit integration of pressure terms.

$$\partial_t(\rho \mathbf{v}) + \nabla p = 0, \tag{32}$$

$$\frac{\gamma - 1}{\gamma}\partial_t(\rho E) + \nabla \cdot (p\mathbf{v}) = 0 \tag{33}$$

$$\begin{tikzcd}
H^1(\Omega) \arrow[r, "\mathrm{grad}"] \arrow[d, "\Pi_0"'] & H(\mathrm{curl}, \Omega) \arrow[d, "\Pi_1"'] \\
V_0 \arrow[r, shift left, "\mathrm{grad}"] & V_1 \arrow[l, shift left, "\mathrm{div}_w"]
\end{tikzcd}$$

First as $p_h \in V_0$, we have $\nabla p_h \in V_1$. So as $\mathbf{m}_h \in V_1$, an implicit Euler discretization in time of equation (49) yields

$$\mathbf{m}_h^{n+1} = \mathbf{m}_h^n - \Delta t \nabla p_h^{n+1} \in V_1.$$

On the other hand, a weak form of (33) reads: Find $p \in V_0$ such that

$$\frac{\gamma - 1}{\gamma}\frac{\mathrm{d}}{\mathrm{d}t}\int \left(\frac{p_h}{\gamma - 1} + \frac{1}{2}\mathbf{u}_h \cdot \mathbf{m}_h\right) q_h - \int \frac{p_h}{\rho}\mathbf{m}_h \cdot \nabla q_h = 0 \quad \forall q_h \in V_0 \tag{34}$$

Discretize in time, linearize and plug in the expression for $\mathbf{m}_h^{n+1}$

$$\frac{1}{\gamma}\int p_h^{n+1,r+1} q_h \,\mathrm{d}\mathbf{x} + \Delta t^2 \int \frac{p_h^{n+1,r}}{\rho^n}\nabla p_h^{n+1,r+1} \cdot \nabla q_h \,\mathrm{d}\mathbf{x} = F^{n,r} \quad \forall q_h \in V_0 \tag{35}$$

symmetric positive definite linear system at each Picard iteration.

(II) Implicit integration of pressure terms: full algorithm

$$\partial_t(\rho \mathbf{v}) + \nabla p = 0, \tag{36}$$

$$\frac{\gamma - 1}{\gamma}\partial_t(\rho E) + \nabla \cdot (p\mathbf{v}) = 0 \tag{37}$$

1. Implicit iterative solve of **symmetric and positive definite** nonlinear system for $p \in V_0$, $\mathbf{m}_f \in V_1$:

$$(\mathbb{M}_0 + \Delta t^2 \mathbb{G}^T \mathbb{M}_1^{\frac{p}{\rho}} \mathbb{G})\mathbf{P}^{n+1,r+1} = \mathbf{H}_{\mathbf{n}}^{n,r}, \tag{38}$$

$$\mathbf{M}_e^{n+1,r+1} = \mathbf{M}_e^m - \Delta t \mathbb{G}\mathbf{P}^{n+1,r+1} \tag{39}$$

2. Update (dual-) barycentric variables $\mathbf{m}^{n+1} = \rho \mathbf{v}^{n+1}$ and ρE^{n+1} with Finite Volume fluxes from Finite Element variables $p^{n+1} \in V_0$ and $\mathbf{m}_e \in V_1$.

$$Q^{**}_{i,j,k} = Q^n_{i,j,k} - \frac{\Delta t}{\Delta x}\left(\mathbf{f}^*_{i+\frac{1}{2},j,k} - \mathbf{f}^*_{i-\frac{1}{2},j,k}\right) \qquad \mathbf{f}^* = \mathbf{f}^*(Q, \mathbf{P}^{n+1,r+1}, \mathbf{M}_e^{n+1,r+1})$$

(III) Implicit and divergence-free integration of the Faraday equation.

$$\partial_t \rho \mathbf{v} - (\nabla \times \mathbf{B}) \times \mathbf{B} = 0 \tag{40}$$
$$\partial_t \mathbf{B} + \nabla \times (-\mathbf{v} \times \mathbf{B} + \eta \nabla \times \mathbf{B}) = 0, \tag{41}$$

- We look for $\mathbf{B}_h \in V_2$ and $\mathbf{m}_h \in V_1$, so that $\nabla \cdot \mathbf{B}_h \in V_3$ is defined *strongly*.
- **Problem (!!)**: this implies $\nabla_w \times \mathbf{B}_h \in V_1$ defined *weakly* .
- **Solution**: **we will split the resistivity term, and solve it on *a new De-Rham complex on a dual-grid*** , for which exist $\tilde{\nabla}$ so that $\tilde{\nabla} \times \tilde{\mathrm{B}}$ is defined strongly (as done in **Fambri2021**).

Resistivity step (strong $curl$):

$$\partial_t \tilde{\mathbf{B}} + \nabla \times \left(\eta \nabla \times \tilde{\mathbf{B}}\right) = 0, \tag{42}$$

ideal-Alfvénic step (strong div):

$$\partial_t \rho \mathbf{v} - (\nabla \times \mathbf{B}) \times \mathbf{B} = 0 \tag{43}$$
$$\partial_t \mathbf{B} + \nabla \times (-\mathbf{v} \times \mathbf{B}) = 0, \tag{44}$$

(III) 1/2 Resistivity step: on a *dual* grid

$$\partial_t \tilde{\mathbf{B}} + \nabla \times \left(\eta \nabla \times \tilde{\mathbf{B}} \right) = 0, \tag{45}$$

$$\begin{tikzcd}
H^1(\Omega) \arrow[r, "\mathrm{grad}"] \arrow[d, "\Pi_0"'] & H(\mathrm{curl}, \Omega) \arrow[r, "\mathrm{curl}"] \arrow[d, "\Pi_1"'] & H(\mathrm{div}, \Omega) \arrow[r, "\mathrm{div}"] \arrow[d, "\Pi_2"'] & L^2(\Omega) \arrow[d, "\Pi_3"'] \\
V_0 \arrow[r, shift left, "\mathrm{grad}"] & V_1 \arrow[l, shift left, "\mathrm{div}_w"] \arrow[r, shift left, "\mathrm{curl}"] & V_2 \arrow[l, shift left, "\mathrm{curl}_w"] \arrow[r, shift left, "\mathrm{div}"] & V_3 \arrow[l, shift left, "\mathrm{grad}_w"]
\end{tikzcd}$$

- We look for $\tilde{\mathbf{B}}_h \in \tilde{V}_1$, so that $\nabla \times \tilde{\mathbf{B}}_h \in \tilde{V}_2$ **is defined strongly** .
- The Galerkin approximation of (45) then reads

$$\frac{\mathrm{d}}{\mathrm{d}t} \int \tilde{\mathbf{B}}_h \cdot \mathbf{C}_h + \int \eta \nabla \times \tilde{\mathbf{B}}_h \cdot \nabla \times \mathbf{C}_h = 0 \; \forall \mathbf{C}_h \in \tilde{V}_1 \tag{46}$$

(III) 1/2 Resistivity step: Time discretization

The semi-discretization in time yields

$$\int \tilde{\mathbf{B}}_h^{n+1} \cdot \tilde{\mathbf{C}}_h + \Delta t \int \eta \nabla \times \tilde{\mathbf{B}}_h^{n+1} \cdot \nabla \times \tilde{\mathbf{C}}_h = \int \tilde{\mathbf{B}}_h^n \cdot \tilde{\mathbf{C}}_h \ \forall \tilde{\mathbf{C}}_h \in \tilde{V}_1 \tag{47}$$

- We notice that the **left-hand-side is a symmetric positive definite bilinear form** .
- then we update the original $\mathbf{B} \in V_2$ via an implicit *strong* Galerkin discretization that reads

$$\mathbf{B}_h^{n+1} + \Delta t \nabla \times \left(P_1(\eta \nabla \times \tilde{\mathbf{B}}_h^{n+1}) \right) = \mathbf{B}_h^n, \tag{48}$$

  Then, by construction $\nabla \cdot \mathbf{B}_h$ **stays zero** if it is zero at the initial time (*strongly*).
- η may eventually account also of numerical stabilization ("*upwind penalization*"), inspired by Multi-Dimensional-Riemann Solvers (see **Balsara2010**);

$$\left\{ [\eta \nabla \times \mathbf{B}]_x \right\}_{i+\frac{1}{2},j,k} := \left[(\eta + s_y^x) \partial_y B_z \right]_{i+\frac{1}{2},j,k} - \left[(\eta + s_z^x) \partial_z B_y \right]_{i+\frac{1}{2},j,k}$$

(III) 2/2 Ideal-Alfvénic step

$$\partial_t(\rho \mathbf{v}) - (\nabla \times \mathbf{B}) \times \mathbf{B} = 0 \tag{49}$$
$$\partial_t \mathbf{B} + \nabla \times (-\mathbf{v} \times \mathbf{B}) = 0, \tag{50}$$

- We look for $\mathbf{B}_h \in V_2$ and $\mathbf{m}_h \in V_1$, so that $\nabla \cdot \mathbf{B}_h \in V_3$ **is defined *strongly*** .
- However $\mathbf{v}_h \times \mathbf{B}_h$ is not in V_1. So we will project it with the orthogonal projection in V_1 that we denote by P_1:
- The Galerkin approximation of (49)-(50) then reads

$$\frac{\mathrm{d}}{\mathrm{d}t} \int \rho \mathbf{v}_h \cdot \mathbf{C}_h + \int \nabla \times P_1(\mathbf{C}_h \times \mathbf{B}_h) \cdot \mathbf{B}_h = 0 \; \forall \mathbf{C}_h \in V_1 \tag{51}$$
$$\frac{\partial \mathbf{B}_h}{\partial t} + \nabla \times P_1 \left(-\mathbf{v}_h \times \mathbf{B}_h\right) = 0 \tag{52}$$

Time discretization

The semi-discretization in time yields respectively

$$\mathbf{B}_h^{n+1} = \mathbf{B}_h^n + \Delta t \nabla \times P_1 \left(\mathbf{v}_h^{n+1} \times \mathbf{B}_h^{n+1} \right) \tag{53}$$

and

$$\int \rho_h \mathbf{v}_h^{n+1} \cdot \mathbf{w}_h + \Delta t \int \nabla \times P_1(\mathbf{w}_h \times \mathbf{B}_h^{n+1}) \cdot \mathbf{B}_h^{n+1} = \int \rho_h \mathbf{v}_h^n \cdot \mathbf{w}_h \ \forall \mathbf{w}_h \in V_1 \tag{54}$$

Let us first observe that $\nabla \cdot \mathrm{B}_h$ **stays zero** if it is zero at the initial time. Indeed, applying a strong divergence to equation (53) we get

$$\nabla \cdot \mathbf{B}_h^{n+1} = \nabla \cdot \mathbf{B}_h^n$$

Implicit equation for $\mathbf{v}_h^{n+1}$

- Plugging (53) into (54) and introducing nonlinear iterations yields

$$\int \rho_h \mathbf{v}_h^{n+1,r+1} \cdot \mathbf{w}_h + \Delta t^2 \int \nabla \times P_1\left(\mathbf{w}_h \times \mathbf{B}_h^{n+1,r}\right) \cdot \nabla \times P_1\left(\mathbf{v}_h^{n+1,r+1} \times \mathbf{B}_h^{n+1,r}\right)$$
$$= -\Delta t \int \nabla \times P_1(\mathbf{w}_h \times \mathbf{B}_h^{n+1,r}) \cdot \mathbf{B}_h^n + \int \rho_h \mathbf{v}_h^n \cdot \mathbf{w}_h \ \forall \mathbf{w}_h \in V_1 \quad (55)$$

- We notice that the **left-hand-side is a symmetric positive definite bilinear form** at each nonlinear iteration.
- This can be solved for $\mathbf{v}_h^{n+1}$ by Picard iterations.
- The nonlinear system for $\mathbf{V}_e$ is decoupled from $\mathbf{B}_f$

Full algorithm for (ideal) Alfvénic subsystem

1. Implicit iterative solve of **symmetric and positive definite** nonlinear system for $\mathbf{V}_e \in V_1$:

$$(\mathbb{M}_2^\rho + \Delta t^2 \mathbb{P}_{B^r}^T \mathbb{C}^T \mathbb{M}_2 \mathbb{C} \mathbb{P}_{B^r}) \mathbf{V}_e^{n+1,r+1} = \mathbf{H}_\mathsf{e}^{n,r}(\mathbf{M}_e^n) \tag{56}$$

   where $\mathbb{P}_{B^r} \mathbf{V}_e^{n+1,r+1}$ is associated to $P_1(\mathbf{v}_h^{n+1,r+1} \times \mathbf{B}_h^{n+1,r})$

2. Update $\mathbf{B}_h^{n+1,r+1}$

$$\mathbf{B}_h^{n+1,r+1} = \mathbf{B}_h^n + \mathbb{C}\mathbb{P}_{B^r} \mathbf{V}_e^{n+1,r+1} \tag{57}$$

3. Update (dual-) barycentric variables $\mathbf{m}^{n+1} = \rho \mathbf{v}^{n+1}$ and ρE^{n+1} with Finite Volume fluxes from Finite Element variables $\mathbf{B}_f^{n+1} \in V_2$.

$$Q_{i,j,k}^{n+1} = Q_{i,j,k}^{**} - \frac{\Delta t}{\Delta x} \left(\mathbf{f}_{i+\frac{1}{2},j,k}^{**} - \mathbf{f}_{i-\frac{1}{2},j,k}^{**} \right) \qquad \mathbf{f}^{**} = \mathbf{f}^{**}(Q, \mathbf{V}_e^{n+1}, \mathbf{B}_h^{n+1})$$

   (momentum and energy conservation)

Time discretization with Operator-Splitting

Given an initial value problem

$$\begin{cases} \frac{dQ}{dt} + A_1(Q) + A_2(Q) = 0, \quad t \in (0, T) \\ Q(0) = Q_0 \end{cases} \tag{58}$$

Defining $X^{n+\theta} = \theta X^{n+1} + (1-\theta)X^n$, the Douglas-Rachford 1956 ($\theta = 1$) scheme or Douglas-Kim (2001; $\theta = \frac{1}{2}$) scheme read as

$$\frac{\hat{Q}^{n+1} - Q^n}{\Delta t} + A_1(\hat{Q}^{n+\theta}) + A_2(Q^n, t^n) = 0 \tag{59}$$

$$\frac{Q^{n+1} - Q^n}{\Delta t} + A_1(\hat{Q}^{n+\theta}) + A_2(Q^{n+\theta}) = 0 \tag{60}$$

In this way the nonlinear implicit system for $(\hat{Q}^{n+1}, A_1)$ is decoupled from (Q^{n+1}, A_2). Note that this algorithm has clearly a *predictor-corrector flavor*.

Following these ideas, we approach a semi-implicit discretization of the nonlinear MHD system

$$\frac{Q^{n+1}-Q^n}{\Delta t} = \mathcal{L}^v(Q^n) + \mathcal{L}^b(Q^{n+\theta_b}) + \mathcal{L}^p(Q^{n+\theta_p})$$

Then we linearize in time in the sense of Picard obtaining

$$\frac{Q^{n+1,r+1}-Q^n}{\Delta t} = \mathcal{L}^v(Q^n) + \hat{\mathcal{L}}^b(Q^{n+\theta_b,r}) \cdot Q^{n+\theta_b,r+1} + \hat{\mathcal{L}}^p(Q^{n+\theta_p,r}) \cdot Q^{n+\theta_p,r+1}, \tag{61}$$

(see also Fambri 2021), and approximate it with the following *recursive* and *operator-splitting algorithm*

$$\frac{\tilde{Q}^{n+1,r+1}-Q^n}{\Delta t} = \mathcal{L}^v(Q^n) + \hat{\mathcal{L}}^b(Q^{n+\theta_b,r}) \cdot \tilde{Q}^{n+\theta_b,r+1} + \hat{\mathcal{L}}^p(Q^{n+\theta_p,r}) \cdot Q^{n+\theta_p,r}, \tag{62}$$

$$\frac{Q^{n+1,r+1,s+1}-Q^n}{\Delta t} = \mathcal{L}^v(Q^n) + \hat{\mathcal{L}}^b(Q^{n+\theta_b,r}) \cdot \tilde{Q}^{n+\theta_b,r+1} + \hat{\mathcal{L}}^p(Q^{n+\theta_p,r,s}) \cdot Q^{n+\theta_p,r+1,s+1}, \tag{63}$$

for $s = 0, \ldots, S$, and $r = 0, \ldots, R$, where r is the recursive Picard index that cycles over the two equations (62-63), while s cycles only over the last equation (63). In the practice, we choose $R = S = 1$. This scheme may recall a recursive *Alternating Direction Implicit* (ADI) method adapted to a three-operator splitting of the type *Explicit-Implicit-Implicit*.

MHD Shock tube problem (Brio-Wu)

initial data $$(\rho, \mathbf{v}, p, \mathbf{B}) = \begin{cases} (\;\;1\;\;,(0,0,0),\;1\;,(\frac{3}{4},+1,0)\sqrt{4\pi}) & x \leq 0 \\ (0.125,(0,0,0),0.1,(\frac{3}{4},-1,0)\sqrt{4\pi}) & x > 0 \end{cases}$$

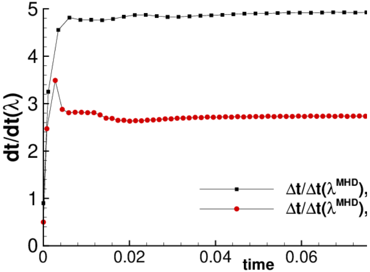

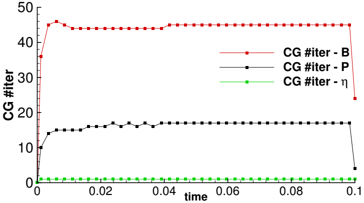

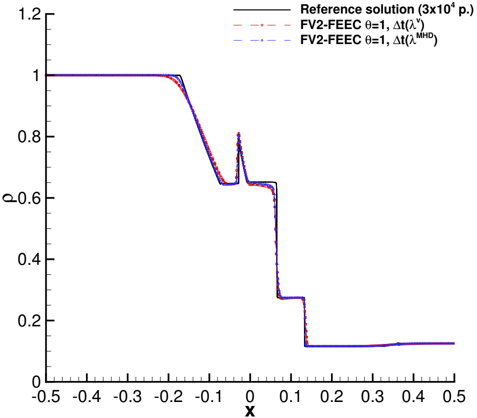

2d tests: low Mach Alfvén-Wave test

- 2^{nd} order of accuracy in space and time with Crank-Nicolson

Low Mach Alfvén-wave test

	N_{element}	L_1 error	L_2 error	L_∞ error	L_1 or.	L_2 or.	L_∞ or.	Th.
ρ	20^2	0.6767E-02	0.3761E-02	0.2936E-02	—	—	—	**2**
	40^2	0.1641E-02	0.9144E-03	0.7123E-03	2.04	2.04	2.04	
	80^2	0.4100E-03	0.2285E-03	0.1789E-03	2.00	2.00	1.99	
	160^2	0.1038E-03	0.5791E-04	0.4558E-04	1.98	1.98	1.97	
u	20^2	0.1485E-01	0.8187E-02	0.6305E-02	—	—	—	**2**
	40^2	0.3820E-02	0.2116E-02	0.1667E-02	1.96	1.95	1.92	
	80^2	0.9620E-03	0.5338E-03	0.4239E-03	1.99	1.99	1.98	
	160^2	0.2420E-03	0.1345E-03	0.1071E-03	1.99	1.99	1.99	
p	20^2	0.6491E-02	0.4171E-02	0.3714E-02	—	—	—	**2**
	40^2	0.1598E-02	0.9965E-03	0.8678E-03	2.02	2.07	2.10	
	80^2	0.4010E-03	0.2463E-03	0.2132E-03	1.99	2.02	2.03	
	160^2	0.1002E-03	0.6176E-04	0.5478E-04	2.00	2.00	1.96	
B_x	20^2	0.4917E-01	0.2744E-01	0.2262E-01	—	—	—	**2**
	40^2	0.1248E-01	0.6981E-02	0.5847E-02	1.98	1.98	1.95	
	80^2	0.3125E-02	0.1751E-02	0.1470E-02	2.00	1.99	1.99	
	160^2	0.7814E-03	0.4381E-03	0.3684E-03	2.00	2.00	2.00	

TABLE 2

L_1, L_2 and L_∞ errors and convergence rates for the low Mach Alfvén wave test.

initial data:

$$
\begin{aligned}
&\rho = 1, \\
&\mathbf{v} = \alpha\left(-n_y\cos(\varphi), n_x\cos(\varphi), \sin(\varphi)\right), \\
&p = 10^2 \\
&B_x = \sqrt{2\pi}\left[n_x + n_y\alpha\cos(\varphi)\right], \\
&B_y = \sqrt{2\pi}\left[n_y - n_x\alpha\cos(\varphi)\right], \\
&B_z = \sqrt{2\pi}\left[-\alpha\sin(\varphi)\right],
\end{aligned}
$$

where

$$\varphi = \frac{2\pi}{n_y}\left[n_x\left(x - n_x t\right) + n_y\left(y - n_y t\right)\right].$$

The direction of propagation is designed in order to be non-aligned with the grid, i.e.

$$\mathbf{n} = \left(n_x, n_y, n_z\right) = (1, 2, 0)/\sqrt{5}.$$

CG iterations

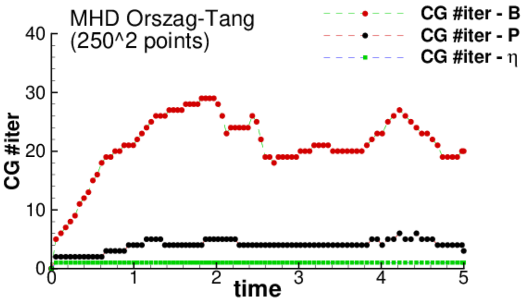

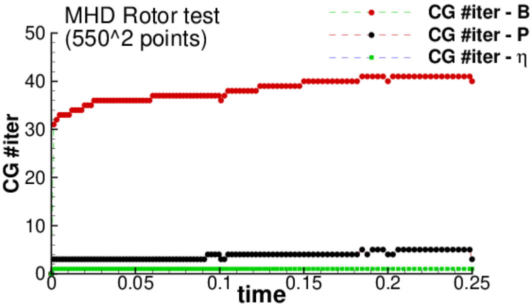

Summary

Semi implicit 3D FV/FEEC scheme for VR-MHD:

- Conservative (mass, momentum and energy);
- Structure preserving (Divergence-free and SYMMETRIC by construction);
- 2^{nd} order accurate;
- Shock-capturing;
- CFL based only on the hydrodynamic convection (flow velocity);
- Nonlinear Solver built as
  - Nested and recursive Picard procedure;
  - symmetric algebraic systems (matrix-free CG method);

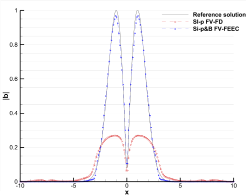

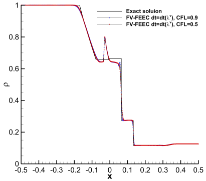

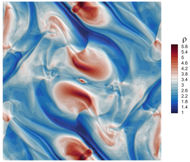

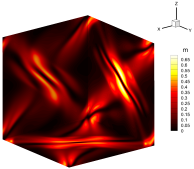

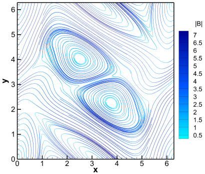

Perspectives

- extension to **high order FV/FEEC or DG/FEEC** (Cartesian grid);
- extension of **DG/FEEC** to realistic curved geometries;
- other physical models (e.g extended MHD, two-fluid MHD);
- (Adaptive) **Mesh Refinement** and **well-balancing**;

Literature

1. **“A structure preserving hybrid finite volume finite element method for compressible MHD”,**
   F. Fambri and E. Sonnendrücker, . [2023, to be submitted]
2. **“A novel structure preserving semi-implicit finite volume method for viscous and resistive magnetohydrodynamics”,**
   Francesco Fambri, (2021), Int. J. for Num. Meth. in Fluids, 93.12, 3447–3489. [`10.1002/fld.5041`]
3. **“A divergence-free semi-implicit finite volume scheme for ideal, viscous, and resistive magnetohydrodynamics”,**
   M. Dumbser, D.S. Balsara, M. Tavelli,F. Fambri, (2019), Int. J. for Num. Meth. in Fluids, 89 (1–2), 16–42. [`10.1002/fld.4681`]
4. **“Flux splitting schemes for the Euler equations”,**
   E.F. Toro, M.E. Vázquez-Cendón, (2012), Computers and Fluids, 70, 1–12. [`arxiv::1808.03788`]
5. **“Multidimensional HLLE Riemann solver: Application to Euler and magnetohydrodynamic flows”,**
   D.S. Balsara, (2010), Journal of Computational Physics, 229, 1970–1993. [`10.3390/axioms7030063`]
6. **“Space-time adaptive ADER-DG schemes for dissipative flows: compressible Navier-Stokes and resistive MHD equations”,**
   F. Fambri, M. Dumbser, and O. Zanotti, (2017), Computer Physics Communications, 220:297–318. [`arXiv:1612.01410`]
7. **“Space-time adaptive ADER discontinuous Galerkin finite element schemes with a posteriori sub-cell finite volume limiting”,**
   O. Zanotti, F. Fambri, M. Dumbser, and A. Hidalgo, (2015), Computers & Fluids, 118:204–224. [`arXiv:1412.0081`]
8. **“Iterative solutions of mildly nonlinear systems”,**
   V. Casulli, P. Zanolli (2012), Journal of Computational and Applied Mathematics, 236 (16), 3937–3947. [`10.1016/j.cam.2012.02.042.`]